

$D \rightarrow \pi\pi$ decays with Final State Interactions

Medina Ablikim^b, Dong-Sheng Du^{a,b}, Mao-Zhi Yang^{a,b}

^a *CCAST(World Laboratory), P.O.Box 8730, Beijing 100080, China*

^b *Institute of High Energy Physics, Chinese Academy of Sciences, P.O.Box 918(4),
Beijing 100039, China*

Abstract

We study $D \rightarrow \pi\pi$ decays with final state interactions considered in one-particle-exchange method. A clear physical picture for final state interactions based on quark and hadronic level diagrams is presented. A strong phase is introduced for hadronic effective couplings, which is crucial for explaining the experimental data of $D^+ \rightarrow \pi^+\pi^0$, $D^0 \rightarrow \pi^+\pi^-$, and $D^0 \rightarrow \pi^0\pi^0$. Rescattering effects between different D decay channels are usually large. They are important for obtaining correct branching ratios for $D \rightarrow \pi\pi$ decays in theoretical calculation.

1 Introduction

The study of heavy meson decays is important for understanding the quark mixing sector of the standard model (SM). It is of great help for determining the quark mixing parameters, searching for the sources of CP violation. However, the quarks in nature are not free, they are bounded in hadrons by strong interactions which are described by nonperturbative QCD. The strong interaction permeates every processes. It almost masks all the information of electroweak (EW) interaction. One must solve the problem of strong interaction before making any meaningful measurements of EW or quark flavor physics in experiment. Solving the problem of nonperturbative QCD needs efforts in both experiment and theory. In the near future BESIII and CLEO-c detector will provide high precision data in charm physics

including data on D meson decays, which will provide the possibility for understanding the physics in charm sector and D decays.

It is the high time to study D meson two-body weak decays beyond the factorization approach now [1]. In general, if a process happens in an energy scale where there are many resonance states, this process must be seriously affected by these resonances [2]. This is a highly nonperturbative effect. Near the scale of D mass many resonance states exist. D meson decays must be affected by them seriously. After weak decays the final state particles rescatter into other particle states through nonperturbative strong interaction [2, 3]. This is called final state interaction (FSI). Every D decay channels can contribute to each other through final state interactions. One can model this rescattering effect as one-particle exchange process [4, 5]. That is to say that the final state particles be scattered into other particle states by exchanging one resonance state existing near the mass scale of D meson. There are also other ways to treat the nonperturbative and FSI effects in nonleptonic D decays. The readers can refer to Ref.[6]

In this paper, we study $D^+ \rightarrow \pi^+\pi^0$, $D^0 \rightarrow \pi^+\pi^-$, and $D^0 \rightarrow \pi^0\pi^0$ decays. We use the one-particle-exchange method to study the final state interactions in these decays. The magnitudes of hadronic couplings needed here are extracted from experimental data on the measured branching fractions of resonances decays. In addition, we introduce a strong phase for the hadronic coupling which is important for obtaining the correct branching ratios of $D \rightarrow \pi\pi$ decays. The coupling constants extracted from experimental data are small for s -channel contribution and large for t -channel contribution. Therefore the s -channel contribution is numerically negligible in $D \rightarrow \pi\pi$ decays. We can safely drop the s -channel contribution in this paper.

The paper is organized as follows. Section II presents the calculation in naive factorization approach. Section III gives the main scheme of one-particle-exchange method. Section IV presents the numerical calculation and discussions. Finally a brief summary is given.

2 Calculations in the factorization approach

We start with the low energy effective Hamiltonian for charm decays [7]

$$\mathcal{H} = \frac{G_F}{\sqrt{2}} \left[\sum_{q=d,s} v_q (C_1 Q_1^q + C_2 Q_2^q) \right], \quad (2.1)$$

where C_1 and C_2 are the Wilson coefficients at m_c scale, v_q is the product of Cabibbo-Kobayashi-Maskawa (CKM) matrix elements and defined as

$$v_q = V_{uq} V_{cq}^*, \quad (2.2)$$

and the current-current operators are given by

$$Q_1^q = (\bar{u}q)_{V-A}(\bar{q}c)_{V-A}, \quad Q_2^q = (\bar{u}_\alpha q_\beta)_{V-A}(\bar{q}_\beta c_\alpha)_{V-A}. \quad (2.3)$$

We do not consider the contributions of the QCD and the electroweak penguin operators in the decays of $D \rightarrow \pi\pi$, since their effects are small in D decays. The values of C_1 and C_2 at m_c scale are taken to be [7]

$$C_1 = 1.126, \quad C_2 = -0.415.$$

In the naive factorization approach, the decay amplitude can be generally factorized into a product of two current matrix elements and can be obtained from (2.1)

$$\begin{aligned} A(D^+ \rightarrow \pi^+ \pi^0) &= -\frac{G_F}{2} V_{ud} V_{cd}^* (a_1 + a_2) i f_\pi (m_D^2 - m_\pi^2) F^{D\pi}(m_\pi^2), \\ A(D^0 \rightarrow \pi^+ \pi^-) &= \frac{G_F}{\sqrt{2}} V_{ud} V_{cd}^* a_1 i f_\pi (m_D^2 - m_\pi^2) F^{D\pi}(m_\pi^2), \\ A(D^0 \rightarrow \pi^0 \pi^0) &= -\frac{G_F}{2} V_{ud} V_{cd}^* a_2 i f_\pi (m_D^2 - m_\pi^2) F^{D\pi}(m_\pi^2), \end{aligned} \quad (2.4)$$

where the parameters a_1 and a_2 are defined as

$$a_1 = C_1 + \frac{C_2}{N_c}, \quad a_2 = C_2 + \frac{C_1}{N_c}, \quad (2.5)$$

with the color number $N_c = 3$. The decay constant f_π and the form factor $F^{D\pi}(0)$ take the values of 0.133 GeV and 0.692 respectively. For q^2 dependence of the form factors, we take the BSW model [1], i.e., the monopole dominance assumption:

$$F(q^2) = \frac{F(0)}{1 - q^2/m_*^2}, \quad (2.6)$$

where m_* is the relevant pole mass.

The decay width of a D meson at rest decaying into $\pi\pi$ is

$$\Gamma(D \rightarrow \pi\pi) = \frac{1}{8\pi} |A(D \rightarrow \pi\pi)|^2 \frac{|\vec{p}|}{m_D^2}, \quad (2.7)$$

where the momentum of the π meson is given by

$$|\vec{p}| = \frac{[m_D^2(m_D^2 - 4m_\pi^2)]^{1/2}}{2m_D}. \quad (2.8)$$

The corresponding branching ratio is

$$Br(D \rightarrow \pi\pi) = \frac{\Gamma(D \rightarrow \pi\pi)}{\Gamma_{tot}}. \quad (2.9)$$

A comparison of the branching ratios of the naive factorization result with the experimental

Table 1: The branching ratios of $D \rightarrow \pi\pi$ obtained in the naive factorization approach and compared with the experimental results.

Decay mode	Br (Theory)	Br (Experiment)
$D^+ \rightarrow \pi^+\pi^0$	3.1×10^{-3}	$(2.5 \pm 0.7) \times 10^{-3}$
$D^0 \rightarrow \pi^+\pi^-$	2.48×10^{-3}	$(1.52 \pm 0.09) \times 10^{-3}$
$D^0 \rightarrow \pi^0\pi^0$	1.0×10^{-7}	$(8.4 \pm 2.2) \times 10^{-4}$

data is presented in Table 1, where the second column gives the pure factorization result. One can notice that the results are not in agreement with the experimental data, especially the second and third decay modes.

3 The one particle exchange method for FSI

As we have seen above, the experimental results for the branching ratios of $D^0 \rightarrow \pi^+\pi^-$ and $D^0 \rightarrow \pi^0\pi^0$ are in disagreement with the calculation from the naive factorization approach. The reason is that the physical picture of naive factorization is too simple, nonperturbative strong interaction is restricted in single hadrons, or between the initial and final hadrons which share the same spectator quark. If the mass of the initial particle is large, such as the case of B meson decay, the effect of nonperturbative strong interaction between the final hadrons most probably is small because the momentum transfer is large. However, in the case of D meson, its mass is not so large. The energy scale of D decays is not very high. Nonperturbative effect may give large contribution. Because there exist many resonances near the mass scale of D meson, it is possible that nonperturbative interaction is propagated by these resonance states, such as, $K^*(892)$, $K^*(1430)$, $f_0(1710)$, etc.

The diagrams of these nonperturbative rescattering effects can be depicted in Figs.1 and 2. The first part $D \rightarrow P_1P_2$ or $D \rightarrow V_1V_2$ represents the direct decay where the decay amplitudes

can be obtained by using naive factorization method. The second part represents rescattering process where the effective hadronic couplings are needed in numerical calculation, which can be extracted from experimental data on the relevant resonance decays.

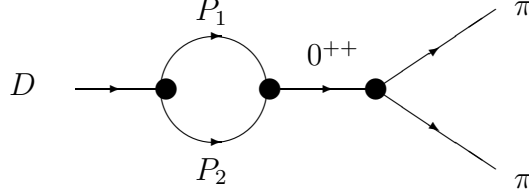


Figure 1: s -channel contributions to final-state interaction in $D \rightarrow \pi\pi$ due to one particle exchange.

Fig.1 is the s -channel contribution to the final state interaction. Here P_1 and P_2 are the intermediate pseudoscalar mesons. The resonance state has the quantum number $J^{PC} = 0^{++}$ derived from the final state particles $\pi\pi$. From Particle Data Group [8], one can only choose $f_0(1710)$ as the resonance state which evaluates the s -channel contribution.

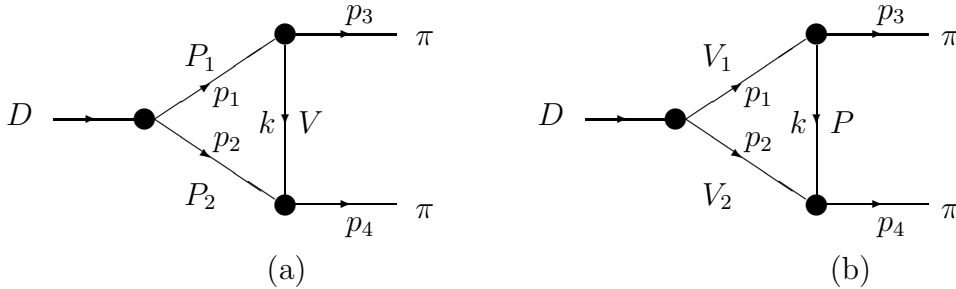


Figure 2: t -channel contributions to final-state interaction in $D \rightarrow \pi\pi$ due to one particle exchange. (a) Exchange a single vector meson, (b) Exchange a single pseudoscalar meson

Fig.2 shows the t -channel contribution to the final state interaction. P_1 , P_2 and V_1 , V_2 are the intermediate states. They rescatter into the final state $\pi\pi$ by exchanging one resonance state V or P . In this paper the intermediate states are treated to be on their mass shell, because their off-shell contribution can be attributed to the quark level. We assume the

on-shell contribution dominates in the final state interaction. The exchanged resonances are treated as a virtual particle. Their propagators are taken as Breit-Wigner form

$$\frac{i}{k^2 - m^2 + im\Gamma_{tot}}, \quad (3.10)$$

where Γ_{tot} is the total decay width of the exchanged resonance.

To the lowest order, the effective couplings of f_0 to PP and VV can be taken as the form

$$L_I = g_{fPP}\phi^+\phi f, \quad (3.11)$$

$$L_I = g_{fVV}A_\mu A^\mu f, \quad (3.12)$$

where ϕ is the pseudoscalar field, A_μ the vector field. Then the decay amplitudes of $f_0 \rightarrow PP$ and VV are

$$T_{fPP} = g_{fPP}, \quad (3.13)$$

$$T_{fVV} = g_{fVV}\epsilon_\mu\epsilon^\mu. \quad (3.14)$$

The coupling constants g_{fPP} and g_{fVV} can be extracted from the measured branching fractions of $f_0 \rightarrow PP$ and VV decays, respectively [8]. Because $f_0 \rightarrow VV$ decays have not been detected yet, we assume their couplings are small. We do not consider the intermediate vector meson contributions in s -channel in this paper.

For the t -channel contribution, the concerned effective vertex is VPP , which can be related to the V decay amplitude. Explicitly the amplitude of $V \rightarrow PP$ can be written as

$$T_{VPP} = g_{VPP} \epsilon \cdot (p_1 - p_2), \quad (3.15)$$

where p_1 and p_2 are the four-momentum of the two pseudoscalars, respectively. To extract g_{fPP} and g_{VPP} from experiment, one should square eqs.(3.13) and (3.15) to get the decay widths

$$\begin{aligned} \Gamma(f \rightarrow PP) &= \frac{1}{8\pi} |g_{fPP}|^2 \frac{|\vec{p}|}{m_f^2}, \\ \Gamma(V \rightarrow PP) &= \frac{1}{3} \frac{1}{8\pi} |g_{VPP}|^2 \left[m_V^2 - 2m_1^2 - 2m_2^2 + \frac{(m_1^2 - m_2^2)^2}{m_V^2} \right] \frac{|\vec{p}|}{m_V^2}, \end{aligned} \quad (3.16)$$

where m_1 and m_2 are the masses of the two final particles PP , respectively, and $|\vec{p}|$ is the momentum of one of the final particle P in the rest frame of V or f . From the above equations, one can see that only the magnitudes of the effective couplings $|g_{fPP}|$ and

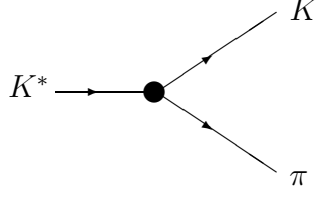


Figure 3: The effective coupling vertex on the hadronic level

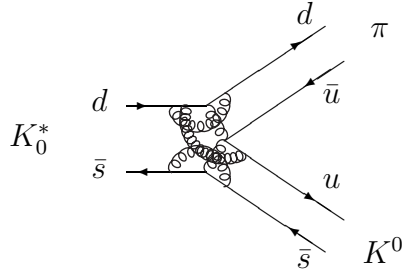


Figure 4: The effective coupling vertex on the quark level

$|g_{VPP}|$ can be extracted from experiment. If there is any phase factor for the effective coupling, it would be dropped. Actually it is quite possible that there are imaginary phases for the effective couplings. As an example, let us see the effective coupling of $g_{K^*K\pi}$ shown in Fig.3, which is relevant to the process $K^* \rightarrow K\pi$. On the quark level, the effective vertex can be depicted as Fig.4, which should be controlled by nonperturbative QCD. From this figure one can see that it is reasonable that a strong phase could appear in the effective coupling, which is contributed by strong interaction. Therefore we can introduce a strong phase for each hadronic effective coupling. In the succeeding part of this paper, the symbol g will only be used to represent the magnitude of the relevant effective coupling. The total one should be $ge^{i\theta}$, where θ is the strong phase coming from Fig.4. For example, the effective couplings will be written in the form of $g_{fPP}e^{i\theta_{fPP}}$ and $g_{VPP}e^{i\theta_{VPP}}$.

The decay amplitude of the s -channel final state interaction can be calculated from Fig.1

$$A_s^{FSI} = \frac{1}{2} \int \frac{d^3\vec{p}_1}{(2\pi)^3 2E_1} \int \frac{d^3\vec{p}_2}{(2\pi)^3 2E_2} (2\pi)^4 \delta^4(p_D - p_1 - p_2) A(D \rightarrow P_1 P_2) \frac{i g_1 g_2 e^{i(\theta_1 + \theta_2)}}{k^2 - m^2 + im\Gamma_{tot}}, \quad (3.17)$$

where p_1 and p_2 represent the four-momenta of the pseudoscalar P_1 and P_2 , the amplitude $A(D \rightarrow P_1 P_2)$ is the direct decay amplitude. The effective coupling constants g_1 and g_2 should be g_{fPP} or g_{VPP} which can be obtained by comparing eq.(3.16) with experimental

data. By performing integrals, we can obtain

$$A_s^{FSI} = \frac{1}{8\pi m_D} |\vec{p}_1| A(D \rightarrow P_1 P_2) \frac{i g_1 g_2 e^{i(\theta_1 + \theta_2)}}{k^2 - m^2 + im\Gamma_{tot}}. \quad (3.18)$$

The t -channel contribution via exchanging a vector meson (Fig.2(a)) is

$$A_{t,V}^{FSI} = \frac{1}{2} \int \frac{d^3 \vec{p}_1}{(2\pi)^3 2E_1} \int \frac{d^3 \vec{p}_2}{(2\pi)^3 2E_2} (2\pi)^4 \delta^4(p_D - p_1 - p_2) A(D \rightarrow P_1 P_2) \\ \times g_1 \epsilon_\lambda \cdot (p_1 + p_3) \frac{i e^{i(\theta_1 + \theta_2)}}{k^2 - m^2 + im\Gamma_{tot}} F(k^2)^2 g_2 \epsilon_\lambda \cdot (p_2 + p_4), \quad (3.19)$$

where $F(k^2) = (\Lambda^2 - m^2)/(\Lambda^2 - k^2)$ is the form factor which is introduced to compensate the off-shell effect of the exchanged particle at the vertices [9]. In the numerical calculation we take $\Lambda = 0.5 \text{ GeV}$. We choose the lightest resonance state as the exchanged particle that gives rise to the largest contribution to the decay amplitude.

We can furthermore obtain

$$A_{t,V}^{FSI} = \int_{-1}^1 \frac{d(\cos \theta)}{16\pi m_D} |\vec{p}_1| A(D \rightarrow P_1 P_2) g_1 \frac{i e^{i(\theta_1 + \theta_2)}}{k^2 - m^2 + im\Gamma_{tot}} F(k^2)^2 g_2 H, \quad (3.20)$$

where

$$H = - \left[m_D^2 - \frac{1}{2}(m_1^2 + m_2^2 + m_3^2 + m_4^2) + (|\vec{p}_1||\vec{p}_4| + |\vec{p}_2||\vec{p}_3|) \cos \theta + E_1 E_4 + E_2 E_3 \right] \\ - \frac{1}{m_V^2} (m_1^2 - m_3^2)(m_2^2 - m_4^2). \quad (3.21)$$

The t -channel contribution by exchanging a pseudoscalar meson (Fig.2(b)) is

$$A_{t,P}^{FSI} = \frac{1}{2} \int \frac{d^3 \vec{p}_1}{(2\pi)^3 2E_1} \int \frac{d^3 \vec{p}_2}{(2\pi)^3 2E_2} (2\pi)^4 \delta^4(p_D - p_1 - p_2) \sum_{\lambda_1, \lambda_2} A(D \rightarrow V_1 V_2) \\ \times g_1 \epsilon_{\lambda_1} \cdot (p_3 - k) \frac{i e^{i(\theta_1 + \theta_2)}}{k^2 - m^2 + im\Gamma_{tot}} F(k^2)^2 g_2 \epsilon_{\lambda_2} \cdot (k + p_4), \quad (3.22)$$

and we obtain

$$A_{t,P}^{FSI} = \int_{-1}^1 \frac{d(\cos \theta)}{16\pi m_D} |\vec{p}_1| \frac{i e^{i(\theta_1 + \theta_2)}}{k^2 - m^2 + im\Gamma_{tot}} X g_1 g_2 F(k^2)^2 (-H_1 + H_2), \quad (3.23)$$

where

$$H_1 = 4im_{V_1} f_{V_1} (m_D + m_2) A_1 \left[\frac{1}{2}(m_D^2 - m_3^2 - m_4^2) \right. \\ - \frac{1}{m_1^2} (E_1 E_3 - |\vec{p}_1||\vec{p}_3| \cos \theta) (E_1 E_4 + |\vec{p}_1||\vec{p}_4| \cos \theta) \\ - \frac{1}{m_2^2} (E_2 E_4 - |\vec{p}_2||\vec{p}_4| \cos \theta) (E_2 E_3 + |\vec{p}_2||\vec{p}_3| \cos \theta) \\ \left. + \frac{1}{2m_1^2 m_2^2} (m_D^2 - m_1^2 - m_2^2) (E_1 E_3 - |\vec{p}_1||\vec{p}_3| \cos \theta) (E_2 E_4 - |\vec{p}_2||\vec{p}_4| \cos \theta) \right], \quad (3.24)$$

$$H_2 = \frac{8im_{V_1}f_{V_1}}{(m_D + m_2)}A_2 \left[E_2E_3 + |\vec{p}_2||\vec{p}_3| \cos \theta - \frac{1}{2m_1^2}(m_D^2 - m_1^2 - m_2^2)(E_1E_3 - |\vec{p}_1||\vec{p}_3| \cos \theta) \right] \\ \left[E_1E_4 + |\vec{p}_1||\vec{p}_4| \cos \theta - \frac{1}{2m_2^2}(m_D^2 - m_1^2 - m_2^2)(E_2E_4 - |\vec{p}_2||\vec{p}_4| \cos \theta) \right], \quad (3.25)$$

and X represents the relevant direct decay amplitude of D decaying to the intermediate vector pair V_1 and V_2 divided by $\langle V_1|(V-A)_\mu|0\rangle\langle V_2|(V-A)^\mu|D\rangle$,

$$X \equiv \frac{A(D \rightarrow V_1V_2)}{\langle V_1|(V-A)_\mu|0\rangle\langle V_2|(V-A)^\mu|D\rangle}.$$

4 Numerical calculation and discussions

In general, every decay channel should be analysed to see whether it can rescatter into $\pi\pi$ state, and how large the contribution is if it can. Here for $D \rightarrow \pi\pi$ decays, the rescattering processes $D \rightarrow \pi\pi \rightarrow \pi\pi$, $D \rightarrow KK \rightarrow \pi\pi$, and $D \rightarrow \rho\rho \rightarrow \pi\pi$, $D \rightarrow K^*K^* \rightarrow \pi\pi$ give the largest contributions, because these intermediate states have the largest couplings with the final state pion and the exchanged meson state shown in Fig.5. The contribution of each diagram in Fig.5 should not only be calculated via eqs.(3.20) and (3.23), there is but also an isospin factor for each diagram which should be multiplied to the calculation of eqs.(3.20) or (3.23). The isospin factor should be considered in such a way that, at first, consider all the possible isospin structure for each diagram in Fig.5 and draw all the possible sub-diagrams on the quark level. One diagram in Fig.5 may amount to several diagrams on quark level. Second, write down the isospin factor for each sub-diagram. For example, the $u\bar{u}$ component in one final meson π^0 contributes an isospin factor $\frac{1}{\sqrt{2}}$, and the $d\bar{d}$ component contributes $-\frac{1}{\sqrt{2}}$. For the intermediate state π^0 , the factor $\frac{1}{\sqrt{2}}$ and $-\frac{1}{\sqrt{2}}$ should be dropped, otherwise, the isospin relation between these three channels $D^+ \rightarrow \pi^+\pi^0$, $D^0 \rightarrow \pi^+\pi^-$ and $D^0 \rightarrow \pi^0\pi^0$ would be violated. Third, sum the contributions of all the possible diagrams on the quark level together to get the isospin factor for each diagram on the hadronic level.

We study these three channels of $D \rightarrow \pi\pi$ decays: $D^+ \rightarrow \pi^+\pi^0$, $D^0 \rightarrow \pi^+\pi^-$ and $D^0 \rightarrow \pi^0\pi^0$. In $D^+ \rightarrow \pi^+\pi^0$, the isospin factors for Fig.5(b) and (d) are zero since the contributions of the sub-diagrams on the quark level cancel each other. The rescattering contribution in $D^+ \rightarrow \pi^+\pi^0$ only depends on $g_{\rho\pi\pi}e^{i\theta_{\rho\pi\pi}}$. In $D^0 \rightarrow \pi^0\pi^0$ decay, however, the FSI contribution only depends on $g_{K^*K\pi}e^{i\theta_{K^*K\pi}}$, because the isospin factors of Fig.5(a) and (c) are zero for the sub-diagrams of them cancel each other. The FSI contribution in $D^0 \rightarrow \pi^+\pi^-$ decay depends on both $g_{\rho\pi\pi}e^{i\theta_{\rho\pi\pi}}$ and $g_{K^*K\pi}e^{i\theta_{K^*K\pi}}$. The numerical results of

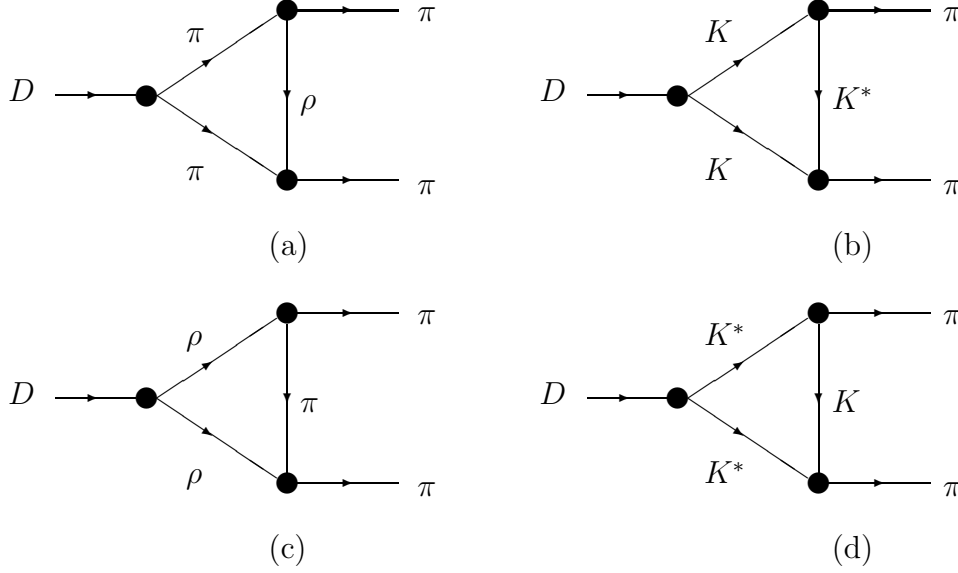


Figure 5: Intermediate states in rescattering process for $D \rightarrow \pi\pi$ decays

the branching ratios of these three $D \rightarrow \pi\pi$ decays including both the direct decay and the rescattering effects are:

$$\begin{aligned}
 Br(D^+ \rightarrow \pi^+\pi^0) &= 1.68 \times 10^{10} | 4.29 \times 10^{-7}i - (6.84 \times 10^{-7} + 8.69 \times 10^{-8}i)e^{i2\theta_{\rho\pi\pi}} |^2, \\
 Br(D^0 \rightarrow \pi^+\pi^-) &= 6.61 \times 10^9 | -6.13 \times 10^{-7}i - (5.41 \times 10^{-7} + 2.43 \times 10^{-8}i)e^{i2\theta_{K^*K\pi}} + \\
 &\quad (9.67 \times 10^{-7} + 1.23 \times 10^{-7}i)e^{i2\theta_{\rho\pi\pi}} |^2, \\
 Br(D^0 \rightarrow \pi^0\pi^0) &= 6.61 \times 10^9 | -3.89 \times 10^{-9}i - (3.82 \times 10^{-7} + 1.72 \times 10^{-8}i)e^{i2\theta_{K^*K\pi}} |^2.
 \end{aligned} \tag{4.26}$$

The above equations satisfy the isospin relation

$$\frac{1}{\sqrt{2}}A(D^0 \rightarrow \pi^+\pi^-) - A(D^0 \rightarrow \pi^0\pi^0) = -A(D^+ \rightarrow \pi^+\pi^0). \tag{4.27}$$

In order to get (4.26), we have used eq.(3.16) and the center value of the measured decay width of $\rho \rightarrow \pi\pi$ and $K^* \rightarrow K\pi$ [8] to obtain $g_{\rho\pi\pi} = 6.0$, $g_{K^*K\pi} = 4.6$. While using the measured value of $f_0(1710) \rightarrow KK$ and $f_0(1710) \rightarrow \pi\pi$ decays [8], one can get $g_{fKK} = 1.6$ and $g_{f\pi\pi} = 0.29$. Comparing the value of g_{fPP} and g_{VPP} , we can see that the amplitude of s-channel contribution to FSI is at least 40 times ($1.6 \times 0.29 / 4.6^2$) smaller than t-channel contribution. Therefore we can drop the s-channel contribution in our numerical analysis. The other input parameters used in the numerical calculation are: 1) the form factors, $F^{D\pi}(0) = 0.692$, $F^{DK}(0) = 0.762$, $A_1^{D\rho}(0) = 0.775$, $A_2^{D\rho}(0) = 0.923$, $A_1^{DK}(0) = 0.880$, $A_2^{DK}(0) = 1.147$

[1]; 2) the decay constants, $f_\pi = 0.133\text{GeV}$, $f_K = 0.158\text{GeV}$, $f_D = 0.205\text{GeV}$, $f_\rho = 0.2\text{GeV}$, and $f_{K^*} = 0.2\text{GeV}$; 3) $\Lambda = 0.5\text{GeV}$.

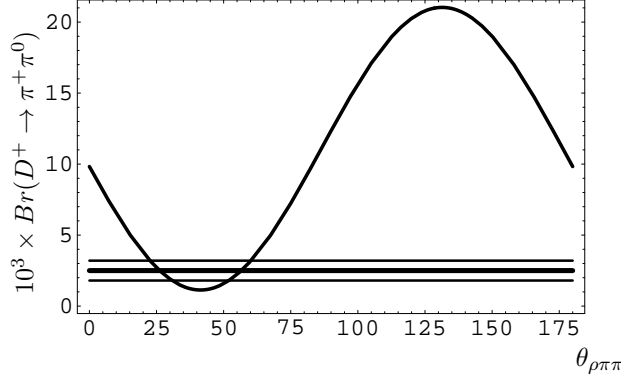


Figure 6: The branching ratio of $D^+ \rightarrow \pi^+\pi^0$ vs. $\theta_{\rho\pi\pi}$. The horizontal lines are the central value of experimental data and error bars.

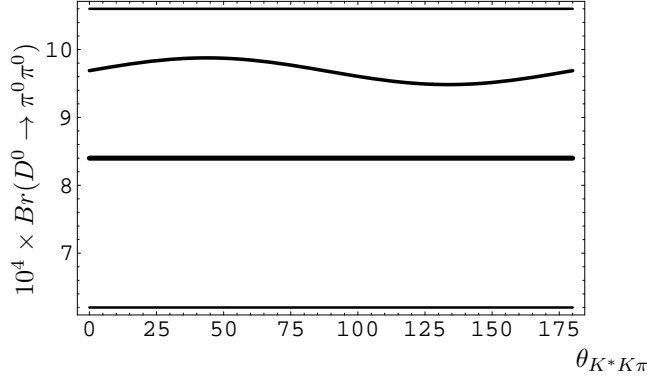


Figure 7: The branching ratio of $D^0 \rightarrow \pi^0\pi^0$ vs. $\theta_{K^*K\pi}$. The horizontal lines are the central value of experimental data and error bars.

The strong phase $\theta_{\rho\pi\pi}$ and $\theta_{K^*K\pi}$ can not be known from any other existing data at present, they are treated as free parameters. Fig.6 and 7 show the branching ratios of $D^+ \rightarrow \pi^+\pi^0$ and $D^0 \rightarrow \pi^0\pi^0$ changing with the strong phase $\theta_{\rho\pi\pi}$ and $\theta_{K^*K\pi}$, respectively. The ranges $(22.6^\circ, 30.8^\circ)$ and $(51.9^\circ, 60.2^\circ)$ for $\theta_{\rho\pi\pi}$ are allowed by the measured branching ratio of $D^+ \rightarrow \pi^+\pi^0$, while the whole range of $\theta_{K^*K\pi}$ is allowed by $D^0 \rightarrow \pi^0\pi^0$. Fig.8 shows the allowed region of $\theta_{\rho\pi\pi}$ and $\theta_{K^*K\pi}$ by the three decay modes $D^+ \rightarrow \pi^+\pi^0$, $D^0 \rightarrow \pi^+\pi^-$ and $D^0 \rightarrow \pi^0\pi^0$. In the overlap regions in Fig.8 all the three decay modes are in agreement with the experimental data. However, if $SU(3)$ symmetry is kept with small violation, the relation $\theta_{\rho\pi\pi} \simeq \theta_{K^*K\pi}$ should be satisfied. Considering this relation, only

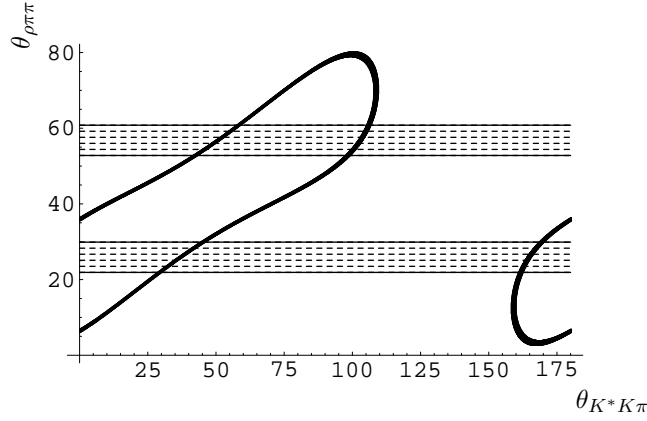


Figure 8: The allowed region of $\theta_{\rho\pi\pi}$ and $\theta_{K^*K\pi}$ by experimental data. The solid belts are from $D^0 \rightarrow \pi^+\pi^-$, and the dashed belts allowed by $D^+ \rightarrow \pi^+\pi^0$. The overlap is allowed by both data.

Table 2: The branching ratios of $D \rightarrow \pi\pi$.

Decay mode	Factorization	Factorization + FSI	Experiment
$D^+ \rightarrow \pi^+\pi^0$	3.1×10^{-3}	2.63×10^{-3}	$(2.5 \pm 0.7) \times 10^{-3}$
$D^0 \rightarrow \pi^+\pi^-$	2.48×10^{-3}	1.57×10^{-3}	$(1.52 \pm 0.09) \times 10^{-3}$
$D^0 \rightarrow \pi^0\pi^0$	1.0×10^{-7}	9.9×10^{-4}	$(8.4 \pm 2.2) \times 10^{-4}$

one of the four overlap regions in Fig.8 shall be allowed, where $51.9^\circ < \theta_{\rho\pi\pi} < 60.2^\circ$ and $40.9^\circ < \theta_{K^*K\pi} < 60.7^\circ$. As an example, Table 2 shows the branching ratios of $D^+ \rightarrow \pi^+\pi^0$, $D^0 \rightarrow \pi^+\pi^-$ and $D^0 \rightarrow \pi^0\pi^0$ by taking one sample point in the overlap region of Fig.8 $(\theta_{\rho\pi\pi}, \theta_{K^*K\pi}) = (57.3^\circ, 51.0^\circ)$, where the $SU(3)$ symmetry violation is in the order of a few degrees. Column ‘Factorization’ is for the branching ratio predicted in naive factorization approach. Column ‘Factorization + FSI’ is for the branching ratio of naive factorization including the final state interaction. The contributions of final state rescattering effects are large, which can improve the predictions of naive factorization to be consistent with the experimental data. The strong phases introduced for the effective hadronic couplings $g_{\rho\pi\pi}$ and $g_{K^*K\pi}$ are important for explaining the experimental data, otherwise, it is quite difficult to get the correct results for the three decay modes at the same time by varying other input parameters.

The parameter Λ in the off-shellness compensating function $F(k^2)$ introduced in eq.(3.19) takes the value 0.5GeV in this calculation, while in Ref.[4, 9] the value takes $\Lambda = 1.2 \sim 2.0\text{GeV}$, that is because it is quite possible that Λ is not an universal parameter. We assume that Λ should be near the masses of the mesons involved in the effective coupling. The

Table 3: The dependence of the branching ratios of $D \rightarrow \pi\pi$ on different values of Λ , where $(\theta_{\rho\pi\pi}, \theta_{K^*K\pi}) = (57.3^\circ, 51.0^\circ)$.

$\Lambda(\text{GeV})$	$D^+ \rightarrow \pi^+\pi^0$	$D^0 \rightarrow \pi^+\pi^-$	$D^0 \rightarrow \pi^0\pi^0$
0.45	9.23×10^{-3}	2.57×10^{-3}	2.2×10^{-3}
0.5	2.63×10^{-3}	1.57×10^{-3}	9.9×10^{-4}
0.55	9.48×10^{-4}	1.39×10^{-3}	4.24×10^{-4}

reaction studied in Ref.[4, 9] is $\bar{P}P \rightarrow \phi\pi$, where the parameter Λ should be near the mass of ϕ meson $m_\phi = 1.02\text{GeV}$. Therefore its value can be taken to be $\Lambda = 1.2 \sim 2.0\text{GeV}$. While in the decay process studied in this paper, K , π , K^* and ρ are involved. Therefore the parameter Λ can take about 0.5GeV , which is located in the range of the masses of these mesons. However, it is still necessary to study the off-shell properties of the hadronic effective couplings in a direct nonperturbative way to check the shape of $F(k^2)$ used in eq.(3.19), because the numerical results of FSI rescattering effects calculated in this model are sensitively dependent on the off-shell properties of the hadronic couplings, or specifically to say, the shape of the off-shell compensating function $F(k^2)$. To show this dependence, we give the results of the three decay branching ratios in Table 3 by varying the value of the parameter Λ . It shows that the branching ratios are very sensitive to the variation of Λ . Certainly there are also many other free parameters, such as the form factors, some meson decay constants which have not yet been well determined in experiment. So the allowed value of the strong phases $\theta_{\rho\pi\pi}$ and $\theta_{K^*K\pi}$ may heavily depends on these parameters. Therefore Fig. 8 shall not be viewed as a stringent constraint on the strong phases. It only shows the possibility to accommodate the three $D \rightarrow \pi\pi$ decay modes consistently in this model. Certainly to completely understand final state interaction, more experimental data and more detailed theoretical works are needed.

Summary We have studied three $D \rightarrow \pi\pi$ decay modes. The total decay amplitude includes direct weak decays and final state rescattering effects. The direct weak decays are calculated in factorization approach, and the final state interaction effects are studied in one-particle-exchange method. The prediction of naive factorization is far from the experimental data. After including the contribution of final state interaction, the theoretical prediction can accommodate the experimental data.

Acknowledgement

This work is supported in part by National Natural Science Foundation of China. M. Yang thanks the partial support of the Research Fund for Returned Overseas Chinese Scholars. M. Ablikim is grateful to Scientific Research Foundation for Returned Scholars of State Education Ministry of China.

References

- [1] M. Wirbel, B. Stech and M. Bauer, *Z. Phys.* **C29**, 637, (1985); M. Bauer, B. Stech and M. Wirbel, *Z. Phys.* **C34**, 103, (1987).
- [2] H.J. Lipkin, *Phys. Rev. Lett.* **44**, 710, (1980); J.F. Donoghue and B.R. Holstein, *Phys. Rev.* **D21**, 1334, (1980).
- [3] J.F. Donoghue, *Phys. Rev.* **D33**, 1516, (1986).
- [4] Y. Lu, B.S. Zou and M.P. Locher, *Z.Phys.* **A345**, 207,(1993); M.P. Locher, Y. Lu and B.S. Zou, *Z.Phys.* **A347**, 281, (1994); Y. Lu and M.P. Locher, *Z.Phys.* **A351**, 83, (1995).
- [5] X.Q. Li and B.S. Zou, *Phys. Lett.* **B399**, 297,(1997); Y.S. Dai, D.S. Du, X.Q. Li, Z.T. Wei and B.S. Zou, *Phys. Rev.* **D60**, 014014, (1999).
- [6] A.N. Kamal and R.C. Verma, *Phys. Rev.* **D35**, 3515, (1987); A.N. Kamal and R. Sinha, *Phys. Rev.* **D36**, 3510, (1987); H.J. Lipkin, *Phys. Lett.* **B 283**, 421, (1992); T.N. Pham, *Phys. Rev.* **D46**, 2976, (1992); L.L. Chau and H.Y. Cheng, *Phys. Lett.* **B333**, 514, (1994); X.Q. Li and B.S. Zou, *Phys. Rev.* **D57**, 1518, (1998).
- [7] G. Buchalla, A.J. Buras and M.E. Lautenbacher, *Rev. Mod. Phys.* **68**, 1125, (1996).
- [8] Particle Data Group, *Eur.Phys. J.* **C**, (2000).
- [9] O. Gortchakov, M.P. Locher, V.E. Markushin and S. von Rotz, *Z. Phys.* **A353**, 447, (1996).